Polarizable bond model for optical spectra of Si(100) reconstructed surfaces

N. Arzate and Bernardo S. Mendoza
Centro de Investigaciones en Optica, A.C., León Guanajuato, México
(Received 8 May 2000; revised manuscript received 14 September 2000; published 28 February 2001)

We calculate the linear and nonlinear optical spectra of clean Si(100)2×1 reconstructed surfaces based on the polarizable bond model. The crystal is treated as an array of pointlike polarizable dipoles in which a dipole replaces each Si-Si bond. The model incorporates the reconstruction of the surface through the local field effect. As a function of the dimer buckling of the 2×1 reconstruction, we calculate the reflectance anisotropy (linear response), and the second-harmonic generation (nonlinear response). We find that a surface with a dimer buckling of 0.6 Å qualitatively reproduces the linear and nonlinear experimental spectra. A number of physical processes, such as charge transfer in the dimer, are explored within this model and compared with experimental results.

DOI: 10.1103/PhysRevB.63.113303 PACS number(s): 78.66.−w, 42.65.An, 42.65.Ky

In recent years optical spectroscopic probes have been of increasing interest in the study of surfaces and interfaces. They do not require ultrahigh vacuum (UHV) environments and are noninvasive, nondestructive, and have wide spectral coverage. Reflectance anisotropy spectroscopy (RAS) is one of the linear optical techniques that is used to characterize structural and electronic properties of semiconductor surfaces.[1] For cubic crystals the bulk optical response is isotropic, so that anisotropies induced by structural changes of the crystal surface can be observed by RAS.[1] On the other hand, second-harmonic generation (SHG) is a sensitive nonlinear optical technique that has been successfully applied to study the surface of centrosymmetric media.[2] SHG arises because the surface and the bulk have different structural symmetry. For materials with inversion symmetry SHG is forbidden (within the dipole approximation) in the bulk, but is allowed at the surface where the inversion symmetry is broken. These two experimental techniques, RAS (Refs. 3–5) and SHG, (Refs. 6–10) have been applied extensively to clean and adsorbate covered Si(100) surfaces, where the atomic structure is formed by asymmetric buckled surface dimers.[11] If the dimers are oriented in the $[01\bar{1}]$ direction, the surface is reconstructed as a 2×1 surface. On the other hand, if the orientation of the buckling angles alternates in the direction perpendicular to the rows, a $c(4\times2)$ reconstruction is obtained.

Several phenomenological and microscopic theoretical methods have attempted to explain the observed RAS and SHG experimental spectra of surfaces and interfaces. The phenomenological RAS models range from the three layer model of McIntyre and Aspnes,[12] the polarizable bond models of Mochán and Barrera,[13] Mendoza and Mochán,[14] Hogan and Patterson,[15] Wijers *et al.*[16] to the more recent microscopic formulations of Mendoza *et al.*,[17] Palummo *et al.*,[18] and Rohlfing and Louie.[19] For surface SHG, the phenomenological polarizable bond model is given in Refs. 14 and 20 and the microscopic formulations are developed in Refs. 21–23. The polarizable bond models have the advantage of having a simple interpretation, and have been successfully applied to Si surfaces.[13–15,20] For instance, the model of Ref. 14 supports the conclusion of Daum *et al.*[7] that the bulk E_1 transition of Si yields a SHG resonance of the clean or oxide covered Si(100) surface due to the vertical strain induced by surface reconstruction. In Ref. 14, the optical spectra were calculated for the unreconstructed surface where the effect of reconstruction was incorporated by a strain induced through a vertical displacement of the first atomic plane. However, the model was not compared with RAS since no experimental data were available.

In this paper, we relax the simple approximation of vertical displacement for inducing the strain, and we apply the polarizable bond model to calculate RAS and SHG spectra of Si(100) for fully relaxed (i.e., reconstructed) surfaces. Within this model the semiconductor crystal is viewed, as an array of pointlike polarizable dipoles with a dipole located at the center of each Si-Si bond since the maximum distribution of charge is located there (see Fig. 1). However, for the bond corresponding to the dimer, the actual position of the dipole may be off centered due to the charge transfer to the upper atom that takes place as the surface reconstructs.[11]

The theoretical development for the linear and the nonlinear response of the polarizable bond model is described in Ref. 14, where the reader is referred for details. However, the following point is discussed here in some detail. The microscopic linear and nonlinear susceptibility tensors of each

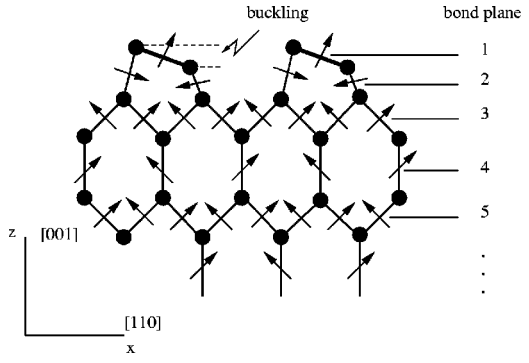

FIG. 1. The 2×1 reconstructed surface of clean Si(100). The arrows represent the pointlike dipoles that replace each Si–Si bond where the dimer has a thicker line. The bond-plane enumeration is also shown.

bond are written in terms of the linear polarizability that depends on position through its particular bond orientation and its surface or bulk location. We consider each dipole to be represented by a cylindrical anisotropic centrosymmetric harmonic oscillator, whose polarizability $\vec{\vec{\alpha}}$ is expressed in terms of the principal polarizabilities $\alpha_{\parallel}$ and $\alpha_{\perp}$, where $\parallel$ ($\perp$) denotes parallel (perpendicular) to the bond. Near the visible spectral region, we expect that the main contributions to $\alpha_{\parallel}$ originate in bonding-antibonding transitions, while $\alpha_{\perp}$ is due mainly to transitions involving atomic states with different symmetry. We assume that the latter has larger resonant frequencies than the former, and we approximate $\alpha_{\perp}$ by a Lorentzian function centered at some relatively high frequency $\omega_{\perp}$ with weight related to ω_p and damping parameter ω_c. Then,

$$\alpha_{\perp}(\omega)=\frac{(f\omega_p)^2}{\omega_{\perp}^2-(\omega+i\omega_c)^2}, \tag{1}$$

where, for the dimer bond, we allow the factor f to be proportional to the amount of charge transfer that takes place to the upper Si of the dimers, as a consequence of surface reconstruction.[11] We take ω_p to have a fixed value, and then the factor $f=1$ is taken for all dipoles except that of the dimer for which $f\geqslant 1$. To obtain $\alpha_{\parallel}(\omega)$, we use

$$\vec{P}(B,\omega)=\frac{\epsilon(\omega)-1}{4\pi}\vec{E}(B,\omega), \tag{2}$$

where $\vec{P}(B,\omega)$ is the total bulk dipole moment, $\vec{E}(B,\omega)$ is the electric field in the bulk, and $\epsilon(\omega)$ is the bulk dielectric function that is determined experimentally. Since $\vec{P}(B,\omega)$ is a function of $\alpha_{\parallel}$ and $\alpha_{\perp}$, Eq. (2) yields an analytical relation between $\vec{\vec{\alpha}}$ and $\epsilon(\omega)$, which is a generalized Clausius-Mossotti relation.[14] Therefore, once $\omega_{\perp}$, ω_p, and ω_c are chosen in Eq. (1), we can solve Eq. (2) for $\alpha_{\parallel}$ for any given $\epsilon(\omega)$ and then we follow the method of Ref. 14 to solve the local-field equations for the linear and nonlinear dipole moments, through which RAS and SHG spectra are calculated.

In our calculations we used three different geometries that are characterized by their dimer buckling. The coordinates of Ref. 24 were used. A zero buckling corresponds to the geometry with symmetric dimers. The values used for the frequency parameters of Eq. (1) are $\hbar\omega_{\perp}=7.05$ eV for both surface (including the dimer) and bulk dipoles, and $\hbar\omega_p=1.68$ eV. These were obtained by finding simultaneously the best agreement with the experimental results of RAS and SHG. The value of $\hbar\omega_{\perp}$ is of the order of the transition energy between the atomic states of Si $3p^2{}^3P$ with $J=0$ and $3d^3D^0$ with $J=1$,[25] in qualitative agreement with the discussion preceding Eq. (1). These parameters are also consistent with those used in Ref. 14. Finally we mention that the results do not depend strongly on ω_c as long as $\omega_c \ll \omega_{\perp}$ (we take $\hbar\omega_c=0.2$ eV) and that a good numerical convergence occurs with ~ 80 crystalline planes.

Figure 2 shows the RAS and SHG spectra of the Si(100)2×1 surface for three surface reconstructions with different buckling, along with the experimental results of Refs. 4 and 5 performed on highly oriented single-domain surfaces for RAS and Ref. 9 performed on double-domain surfaces for SHG. All dipoles (including the dimers) are taken to have identical $\vec{\vec{\alpha}}(\omega)$, with $f=1$. For RAS we observe the following features. All theoretical spectra show three features above 3.5 eV that are near the experimentally determined values of 3.6, 4.3, and 5.3 eV. However, only the surface with a buckling of 0.7 Å gives the RAS features having correct signs at 3.9 and 4.2 eV, in qualitative agreement with experiment. The RAS spectrum for the surface with symmetric dimers shows a feature at 3.3 eV in correspondence with the experimental one at the same energy. However this case also shows a broad and large negative structure at 2.4 eV not seen in the experimental curves. In addition, only the RAS spectrum of the geometry with buckling of 0.6 Å has a feature at 1.5 eV, which qualitatively reproduces the experimental one at 1.6 eV. Similar results at 1.5 and 4.3 eV are reported in Ref. 18 but the RAS spectra calculated there have several features between 1.5 and 4.0 eV that are not present in the experimental data and in our spectra.

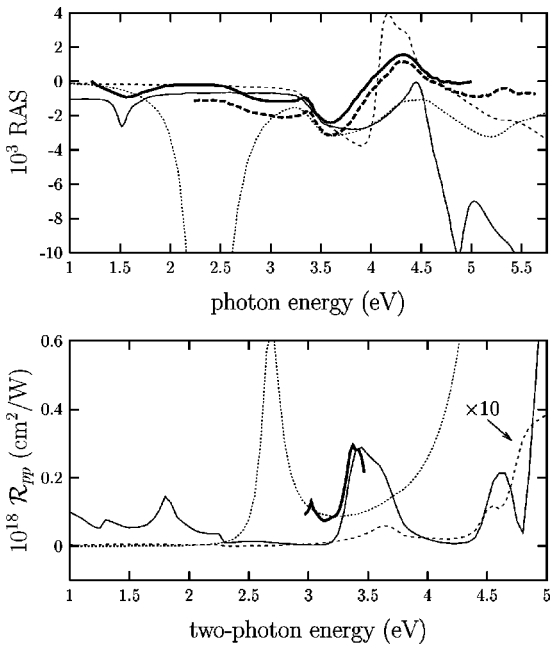

FIG. 2. (Top panel) RAS spectra and (bottom panel) SHG spectra for *p*-in *p*-out polarizations, of clean Si(100)2×1, for different dimer bucklings: 0 Å (symmetric dimers) (dotted line), 0.6 Å (thin-solid line), and 0.7 Å (dashed line). The experimental spectra are also shown: for RAS the thick-solid line is from Ref. 4 and the thick-dashed line is from Ref. 5; for SHG the thick-solid line (rescaled on the vertical axis) is from Ref. 9. We mention that the vertical scale for SHG is within the same order of magnitude as the microscopic calculation of Ref. 21.

Moving to SHG we obtained the results of Figs. 2 and 3 where we have shifted the theoretical curves upward by 0.3 eV to provide better correspondence between calculated and measured structures. We see from Fig. 2 that for the surface with a buckling of 0.6 Å, the E_1 resonance seen experimentally at 3.4 eV (in the two-photon energy) is reproduced. At 4.6 eV there is another peak that corresponds to the bulk E_2 Si transition. Also, for this surface there is a peak at 1.8 eV.

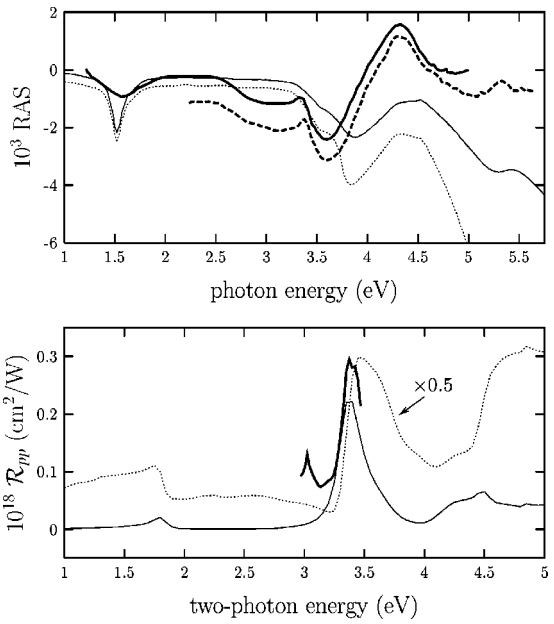

FIG. 3. Same as Fig. 2, for a dimer buckling of 0.6 Å. The dotted line is for $\Delta=0$, whereas the thin-solid line is for $\Delta=0.25a$, which gives the dimer's dipole displaced towards the upper Si by 0.25 of its length. Both spectra have the same $f=1.9$.

For the surface with a buckling of 0.7 Å, the E_1 peak appears, but it is now blueshifted in comparison with that of the previous surface, and the E_2 peak is seen as a small shoulder slightly redshifted with respect to the same previous surface. Further, the intensity of its spectrum is an order of magnitude smaller than for 0.6 Å. For zero buckling, we find that the E_1 peak is strongly redshifted to 2.7 eV, and E_2 is also strongly blueshifted to 5 eV, which is not shown in the plot since it has a large intensity. The qualitative dependence of the SHG E_1 resonance with respect to the buckling of the dimer is also seen in the microscopic model of Ref. 26. Thus, our results may imply that if the local field is incorporated into a microscopic calculation, one should expect the SHG resonant peaks to shift. Finally we mention that neither case reproduces the surface peak at 3 eV seen in the experimental curve. This peak is obtained in the microscopic theory of Ref. 21 and is due to electronic surface states related to the dimer.[27] Since we have treated the dipole corresponding to the dimer's bond in the same manner as (except for its orientation) a bulk bond, we should not expect to have a surface related transition.

In principle one should be able to chose an appropriate $\vec{\vec{\alpha}}(\omega)$ for the dimer and surface bonds in order to reproduce the surface SHG peak at 3 eV. However, we would like to keep the number of adjustable parameters to a minimum, and instead try to look into the phenomenology that the present model allows in simple physical terms, and see its consequences in the RAS and SHG spectra. Therefore, in what follows, we explore an interesting point related to the prediction of Chadi by which, in a tilted dimer, there is a charge transfer of $\sim e/3$ into the upper Si atom of each buckled dimer.[11] In order to include such a charge transfer in our model, we can adjust the following two variables: (a) f for the dimer alone [see Eq. (1)], since it is proportional to the dimer electronic density, and (b) the position of the point dipole that replaces the dimer's bond, from its nominal centered position $\Delta=0$, to an off-centered position $\Delta\neq 0$, since the charge is redistributed in the same manner as its centroid. We have done such an exploration for the surface with a buckling of 0.6 Å, and have found that the best RAS and SHG are given by $f=1.9$ and $\Delta=0.25a$ towards the upper Si atom of the dimer where a is the dimer's bond length. Both values are consistent with the Chadi's prediction of charge transfer. We show in Fig. 3 the RAS and SHG spectra for such values of f and Δ. Comparing the spectra, we see that $\Delta=0.25a$ gives a much better line shape than $\Delta=0$ (whose spectrum is larger by a factor of 2), since the RAS feature at 1.5 eV and the SHG peak E_2 at 4.5 eV are very well defined. Also, the RAS spectrum qualitatively reproduces the small feature seen in the experiment of Ref. 5 above 5 eV. On the other hand, if we use a negative Δ, which would imply an off-centered dipole towards the lower Si atom in the dimer, we obtain RAS and SHG spectra that do not agree with experiment, thus confirming the prediction of Chadi through this optical model.[11]

To understand the origin of the structure shown in the above spectra, we proceed as follows. The solution of the total dipole moment that represents the polarization of the system has the following structure:[28,29]

$$p(n\omega)\sim\frac{S(n\omega)}{1-\alpha(n\omega)M}\sim\mathcal{E}(n\omega)S(n\omega), \tag{3}$$

where $n=1,2$ refers to the linear or nonlinear solution, respectively. We identify the local field $\mathcal{E}$ as $\mathcal{E}(n\omega)\sim[1-\alpha(n\omega)M]^{-1}$ and $S(\omega)$ as the linear source proportional to the external perturbing field. On the other hand, $S(2\omega)$ is the nonlinear source proportional to $\mathcal{E}^2(\omega)$, with M representing the dipolar interaction tensor, and $\alpha(\omega)$ representing $\vec{\vec{\alpha}}(\omega)$.[14] From Eq. (3), $p(\omega)$ could have structure only from the local field $\mathcal{E}$ at ω, since $S(\omega)$ has no structure. In contrast, $p(2\omega)$ could have structure at 2ω directly from $\mathcal{E}(2\omega)$, and also through $S(2\omega)$, which is driven by the local field $\mathcal{E}$ at ω. For instance, we have checked that in Fig. 3 the SHG peak at $2\hbar\omega=1.8$ eV comes from the local field $\mathcal{E}$ at 2ω, and that the SHG E_1 peak comes from the local field $\mathcal{E}$ at ω (through the nonlinear source), just as the RAS feature at 1.5 eV also comes from the local field $\mathcal{E}$ at ω.[30]

Within this model, we also find that the dominant interaction of the dimer with the subsurface bonds comes from the ones corresponding to the third through the fifth bond layers (see Fig. 1). Indeed, we have checked that if the interaction of the dimer with any of these layers is artificially set to zero, the 1.5 eV feature in RAS and the E_1 peak in SHG disappear. These results show clearly how RAS and SHG are sensitive to the surface and subsurface region.[31]

Finally, to compare with other reconstructions, we have calculated RAS and SHG for a $c(4\times2)$ surface reconstruction and for an ideally terminated (100) surface. We find that the RAS spectrum of the $c(4\times2)$ does not reproduce the experimental results as good as the 2×1 reconstruction does for a surface with a buckling of 0.6 Å. However, for SHG

we find E_1 (E_2) with larger (smaller) intensity than the 2×1 case, and also the surface experimental peak at 3 eV is not present. For the ideally terminated (100) surface we find a finite RAS spectrum. On the other hand, the SHG spectrum has no E_1 peak, thus confirming the statement that the surface reconstruction gives rise to the observed nonlinear spectra.

In summary, we have applied the model of polarizable bonds to study the surface RAS and SHG optical spectra of clean Si(100)2×1. We find that both RAS and SHG are sensitive to the buckling of the dimer and that, a surface with dimer buckling of 0.6 Å qualitatively reproduces most of the experimental features reported in the literature. By changing parameters of the model, we conclude that the structures in RAS and SHG are produced by the atomic reconstruction of the surface through the local field induced in the surface and subsurface region. We calculated also the spectra for a $c(4\times2)$ surface reconstruction and found that, although it produces a SHG E_1 resonance, its agreement with RAS is not as good as that of the 2×1 reconstruction. This might suggest a combination of both reconstructions in the experimental sample. The surface sensitivity shown by this model is such that, as a further extension of this paper, one can refine the dimer geometry by varying structural parameters and by choosing a few frequencies, like E_1 and E_2, at which to fit the spectral features of RAS and SHG. However, this is beyond the scope of this paper. In order to make a direct comparison with such theoretical results, the same sample should be studied in RAS and SHG spectroscopic experiments.

We acknowledge the partial support of CONACyT-México (26651-E).

[1] R. Del Sole, in *Photonics Probes*, edited by P. Halevi (Elsevier, Amsterdam, 1995), p. 131, and references therein.
[2] G. Lüpke, Surf. Sci. Rep. **35**, 75 (1999).
[3] T. Yasudas, T. Yasuda, L. Mantese, U. Rossow, and D. E. Aspnes, Phys. Rev. Lett. **74**, 3431 (1995).
[4] R. Shioda and J. van der Weide, Phys. Rev. B **57**, R6823 (1998).
[5] S. G. Jaloviar, Jia-Ling Lin, Feng Liu, V. Zielasek, L. McCaughan, and M. G. Lagally, Phys. Rev. B **82**, 791 (1999).
[6] J. F. McGilp, Surf. Rev. Lett. **6**, 529 (1999).
[7] W. Daum, W. Daum, H.-J. Krause, U. Reichel, and H. Ibach, Phys. Scr. **T49**, 513 (1993); Phys. Rev. Lett. **71**, 1234 (1993).
[8] U. Höfer, Appl. Phys. A: Mater. Sci. Process **63**, 533 (1996).
[9] J. I. Dadap, Z. Xu, X. F. Hu, M. C. Downer, N. M. Russell, J. G. Ekerdt, and O. A. Aktsipetrov, Phys. Rev. B **56**, 13 367 (1997).
[10] D. Lim, M. Downer, J. Ekerdt, N. Arzate, B. Mendoza, V. Gavrilenko, and R. Wu, Phys. Rev. Lett. **84**, 3406 (2000).
[11] D. J. Chadi, Phys. Rev. Lett. **43**, 43 (1979); W. X. Verwoerd, Surf. Sci. **99**, 581 (1980).
[12] J. D. E. McIntyre and D. E. Aspnes, Surf. Sci. **24**, 417 (1971).
[13] W. L. Mochán and R. G. Barrera, Phys. Rev. Lett. **55**, 1192 (1985); **56**, 2221 (1986).
[14] B. S. Mendoza and W. L. Mochán, Phys. Rev. B **55**, 2489 (1997).
[15] C. D. Hogan and C. H. Patterson, Phys. Rev. B **57**, 14 843 (1998); C. H. Patterson and D. Herrendörfer, J. Vac. Sci. Technol. A **15**, 3036 (1997); D. Herrendörfer and C. H. Patterson, Surf. Sci. **375**, 210 (1997).
[16] C. M. J. Wijers, P. L. de Boeij, C. W. van Hasselt, and Th. Rasing, Solid State Commun. **93**, 17 (1995).
[17] B. S. Mendoza, R. Del Sole, and A. Shkrebtii, Phys. Rev. B **57**, R12 709 (1998).
[18] M. Palumno, G. Onida, R. Del Sole, and B. S. Mendoza, Phys. Rev. B **60**, 2522 (1999).
[19] M. Rohlfing and S. G. Louie, Phys. Rev. Lett. **83**, 856 (1999).
[20] B. S. Mendoza and W. L. Mochán, Phys. Rev. B **53**, R10 473 (1996); W. L. Schaich and B. S. Mendoza, *ibid.* **45**, 14 279 (1992).
[21] B. S. Mendoza, A. Gaggiotti, and R. Del Sole, Phys. Rev. Lett. **81**, 3781 (1998).
[22] V. I. Gavrilenko, R. Q. Wu, M. C. Downer, J. G. Ekerdt, D. Lim, and P. Parkinson, Thin Solid Films **364**, 1 (2000).
[23] B. S. Mendoza, M. Palumno, G. Onida, and R. Del Sole (unpublished).
[24] For 0 and 0.7 Å we used A. Ramstad, G. Brocks, and P. J. Kelly, Phys. Rev. B **51**, 14 504 (1995), and for 0.6 Å we used R. M. Tromp, R. G. Smeenk, F. W. Saris, and D. J. Chadi, Surf. Sci. **133**, 137 (1983).
[25] Charlotte E. Moore, *Atomic Energy Levels* (National Bureau of Standards, Washington, DC, 1970), p. 144.
[26] B. S. Mendoza, A. Gaggiotti, and R. Del Sole, Phys. Status Solidi A **170**, 343 (1998).
[27] N. Arzate and B. S. Mendoza, Phys. Rev. B (to be published).
[28] A. Guerrero and B. S. Mendoza, J. Opt. Soc. Am. B **12**, 559 (1995); B. S. Mendoza, Opt. Rev. **1**, 223 (1994).
[29] J. Cruz and B. S. Mendoza, Phys. Rev. B **62**, 8438 (2000).
[30] We mention that double resonances where $S(2\omega)$ and $\mathcal{E}(2\omega)$ resonate at the same frequency producing a huge enhancement of the SHG yield, could be found in other type of structures by adjusting the geometry of the system as shown in Ref. 28.
[31] Similar qualitative results are found in the microscopic treatment of Ref. 27, in which the electronic transitions are between dimer and subsurface electronic states.